MDPI

Article

Characteristics of Observed Electromagnetic Wave Ducts in Tropical, Subtropical, and Middle Latitude Locations

Sandra E. Yuter [1,‡,*], McKenzie M. Sevier [1,‡], Kevin D. Burris [1,†,‡] and Matthew A. Miller [1,‡]

[1] Department of Marine, Earth, and Atmospheric Sciences, North Carolina State University, Raleigh, NC, USA
[*] Correspondence: seyuter@ncsu.edu
[†] Current address: Department of Physics and Meteorology, US Air Force Academy, Colorado Springs, CO, USA.
[‡] These authors contributed equally to this work.

Abstract: Where and at what altitudes electromagnetic wave ducts within the atmosphere are likely to occur is important for a variety of communication and military applications. We examine the modified refractivity profiles and wave duct characteristics derived from observed upper air soundings obtained over four years from 7 tropical and subtropical islands, and middle latitude sites at 4 US coastal locations, 3 sites near the Great Lakes, and 4 US inland sites. Across all location types, elevated ducts are more common than surface-based ducts and median duct thicknesses are ∼100 m. There is a weak correlation between duct thickness and strength and essentially no correlation between duct strength and duct base height. EM ducts more frequently occur at the tropical and subtropical island locations (∼60%) and middle latitude coastal locations (70%) as compared to less than 30% of the time at the Great Lake and US inland sites. The tropical and subtropical island sites are more likely than the other location types to have ducts at altitudes higher than 2 km which is above the boundary layer height.

Keywords: modified refractivity; wave duct; trapping layer; upper air sounding

0. Introduction

Atmospheric refraction bends electromagnetic (EM) waves when the waves traverse gradients in temperature and humidity[1–4]. In general, the refractive index in Earth's atmosphere decreases with increasing height and as a consequence beam paths bend downward relative to the surface compared to their path in a vacuum. Profiles of refractive index permit calculation of EM beam paths. In some weather conditions, stable layers can occur and yield adjacent atmospheric layers with distinct temperature and humidity characteristics and sharp gradients in refractive index. In these circumstances, the beam paths can be ducted wherein the waves are guided within a horizontal layer which allows them to travel further than they would in normal conditions. Temperature inversions, where temperature increases with increasing altitude, can yield trapping layers within ducts if the gradients in temperature and humidity are strong enough. Ducting can be caused by subsidence aloft, boundary layer inversions, or cooling near the surface such as by nocturnal radiation inversions over land or warm dry air moving over a cooler body of water. In calm, stable conditions over ocean, air in contact with the sea surface can become saturated yielding ducting conditions ∼10 m in thickness [4]. Evaporative downdrafts from precipitating clouds can also yield trapping layers at any altitude below cloud base. Surface cold pools originating from evaporative downdrafts will spread laterally so trapping layers associated with them will vary in height with time. Globally, the highest ducting probabilities are found in the Arabian Sea and in marine stratocumulus conditions in the subtropics [5].

Previous work has extensively addressed the theory of EM refraction [1,2,4,6]. The characteristics of ducts have been the focus of many studies using both observations and

Citation: Lastname, F.; Lastname, F.; Lastname, F. Title. *Atmosphere* **2024**, *1*, 0. https://doi.org/

Received:
Revised:
Accepted:
Published:

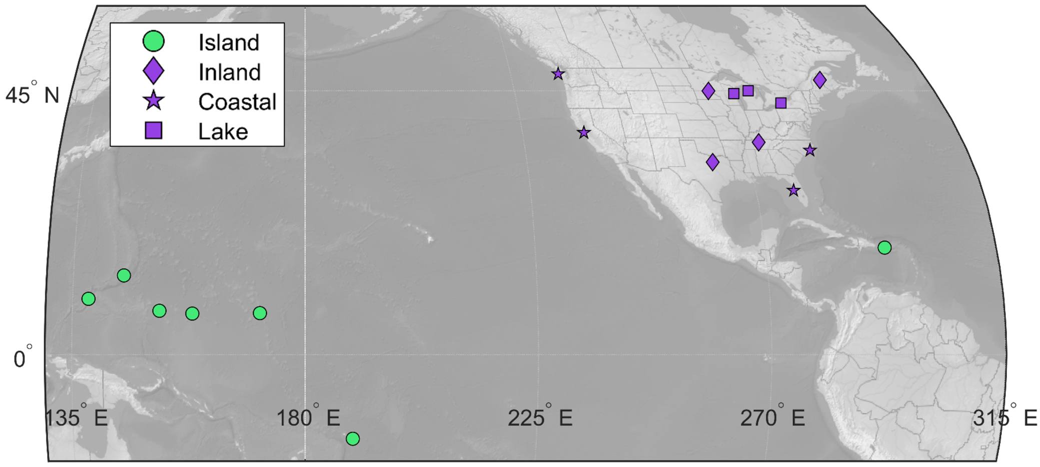

Figure 1. Locations of upper air sounding data used for refractivity profile EM duct analysis. Location type is distinguished by marker type. Color indicates groupings of a location type.

Table 1. Upper air sounding sample sizes and total duct counts for ducts with >40 m thickness and M > 1.7 at 18 locations over 4 years (2019-2022) by location type.

Location Type:	Total Soundings:	# of soundings with ≥ 1 duct:	Percent of soundings with ≥ 1 duct:	Duct Count:
Island	19,524	11,538	59.1%	32,352
Coastal	8,850	6,338	71.6%	12,938
Lake	8,871	2,367	26.7%	3,508
Inland	11,992	3,565	29.7%	5,403

modeling [e.g. 7–14]. Other work has utilized inversion methods which estimate refractivity profiles from the measured signal and wave propagation models [e.g. 15]. In this paper, we address the prevalence and characteristics of observed ducts both at the surface and aloft using a high vertical resolution (∼5 m) upper air sounding data set. These high resolution soundings provide new details on shallow ducting layers in the atmosphere that are not possible to resolve with lower vertical resolution observations or model output [e.g. 5]. Information on the geography and altitudes of frequent refractivity conditions conducive for ducting is useful for navigation, communication, weather radar, as well as defensive and offensive military applications [6,11].

1. Materials and Methods

We use upper air soundings with a native vertical resolution of ∼5 m from selected sites in the United States, its territories, and several Pacific islands. Data are from the period 1 January 2019 to 31 December 2022. In total, atmospheric profiles were analyzed for 49,239 upper air soundings, 23,806 of which contained one or more ducts (Table 1). We analyze profiles from 7 island sites, 4 coastal sites, 3 sites around the Great Lakes, and 4 inland sites (Fig. 1, Table 2). These categories represent varying geographic settings which influence atmospheric properties and ducting behavior. At coastal locations, offshore flow and along-shore flow can yield surface-based ducts and onshore flow can yield both surface-based and ducts aloft [9]. Previous work has not examined observed duct characteristics at multiple tropical island locations. While the lowest sounding levels are island influenced, once the sounding is a few km downwind of the island, the conditions are more representative of open ocean.

The sounding data are archived by the National Centers for Environmental Information (NCEI) in Binary Universal Form for the Representation of meteorological data (BUFR)

Table 2. Upper air sounding locations subset into corresponding location type: tropical and subtropical island, US coastal, Great Lake, and US inland respectively. Latitude and longitude coordinates and local times at 00 and 12 UTC are listed for each location. For sites that participate in daylight savings, the first local time listed is daylight standard time and the second is daylight savings time.

Location Name	Latitude (°)	Longitude (°)	Local time at 00 UTC	Local time at 12 UTC
Island				
American Samoa	-14.33	-170.71	1300	0100
Chuuk	7.46	151.84	1000	2200
Guam	13.48	144.80	1000	2200
Marshall Islands	7.06	171.27	1200	0000
Micronesia	6.99	158.21	1100	2300
Puerto Rico	18.22	-66.59	2000	0800
Yap	9.50	138.08	1000	2200
Coastal				
Oakland, CA	37.80	-122.27	1600/1700	0400/0500
Newport, NC	34.79	-76.86	1900/2000	0700/0800
Quilayute, WA	47.94	-124.54	1600/1700	0400/0500
Tampa, FL	27.95	-82.46	1900/2000	0700/0800
Lake				
Buffalo, NY	42.89	-78.88	1900/2000	0700/0800
Gaylord, MI	45.03	-84.67	1900/2000	0700/0800
Green Bay, WI	44.51	-88.01	1800/1900	0600/0700
Inland				
Caribou, ME	46.86	-68.00	1900/2000	0700/0800
Fort Worth, TX	32.76	-97.33	1800/1900	0600/0700
Minneapolis, MN	44.98	-93.27	1800/1900	0600/0700
Nashville, TN	36.16	-86.78	1800/1900	0600/0700

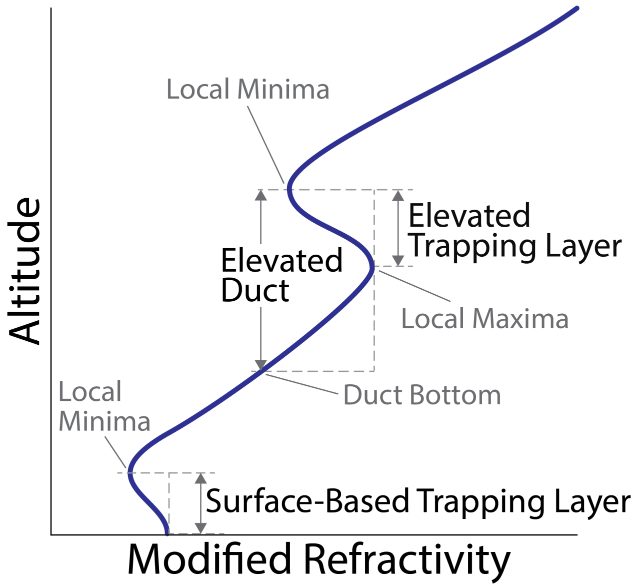

Figure 2. Idealized schematic of electromagnetic wave duct components as a function of modified refractivity and height. Adapted from [9].

format [16,17]. Operational upper air soundings are launched at ∼11 UTC and ∼23 UTC to achieve mid troposphere altitudes at 0 and 12 UTC each day. The data set we use spans 10 time zones, yielding differences in local times among the sites (Table 2). We do not have adequate temporal sampling to analyze diurnal cycle variations.

The observed upper air sounding profiles at ∼5 m native resolution are linearly interpolated to 20 m vertical layers and then input to the calculation of modified refractivity (M). Modified refractivity is a function of temperature, water vapor, pressure and the curvature of the Earth. The advantage of modified refractivity over refractivity is that all negative M vertical gradients are associated with trapping layers which simplifies duct identification[4,15]. Modified refractivity (M) is determined using the following equation:

$$M = \frac{77.6}{T}(P + \frac{4810e}{T}) + \frac{z}{10^{-6}R_e} \tag{1}$$

where P is pressure (mb), T is temperature (K), e is vapor pressure (mb), z is height (m) and R_e is the radius of the Earth (m) [2,7]. Modified refractivity values are calculated for each height level in each sounding.

Figure 2 illustrates the key components and characteristics of a wave duct as a function of modified refractivity and altitude. A trapping layer is characterized by a decrease in modified refractivity with increasing height [9]. The thickness of an elevated duct is the distance between the local minimum in M above the trapping layer to the same value of M below the trapping layer. Surface-based ducts only have the trapping layer portion in which case the duct thickness is defined as the trapping layer thickness. Observed examples of modified refractivity profiles are annotated with trapping layer top and bottom and duct base in Figure 3. The example from Guam at 1106 UTC on 31 March 2022 contains seven ducts aloft (Fig. 3a). A surface duct along with three ducts aloft is shown in the example from Wallops Island, VA, at 2300 UTC on 11 July 2022 (Fig. 3b).

Using the information on trapping layer top and bottom and duct base, we calculate duct strength as the difference between the local maxima in M at the trapping layer bottom and local minima in M at the trapping layer top. Two thresholds were applied to filter out very weak or very thin modified refractivity inversions. A duct was included in the analysis only if it met both the criteria of duct strength M> 1.7 and duct thickness > 40 m. By focusing on these features, this study aims to provide improved understanding of electromagnetic wave duct frequency of occurrence and variations across different environments.

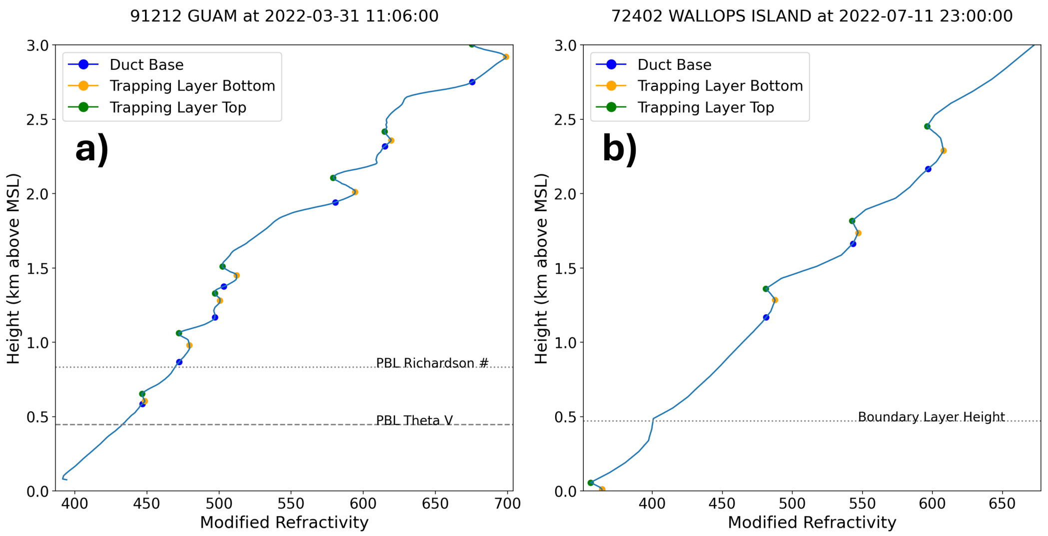

Figure 3. Modified refractivity profiles from a) Guam on 1106 UTC 31 March 2022 with multiple ducts aloft and b) Wallops, VA on 2300 UTC 11 July 2022 with multiple ducts aloft and a surface duct. Planetary boundary layer height based on Richardson number and on virtual potential temperature (Theta V) [18] differed in a) and are shown separately. In b) both estimates of the boundary layer height were at the same altitude.

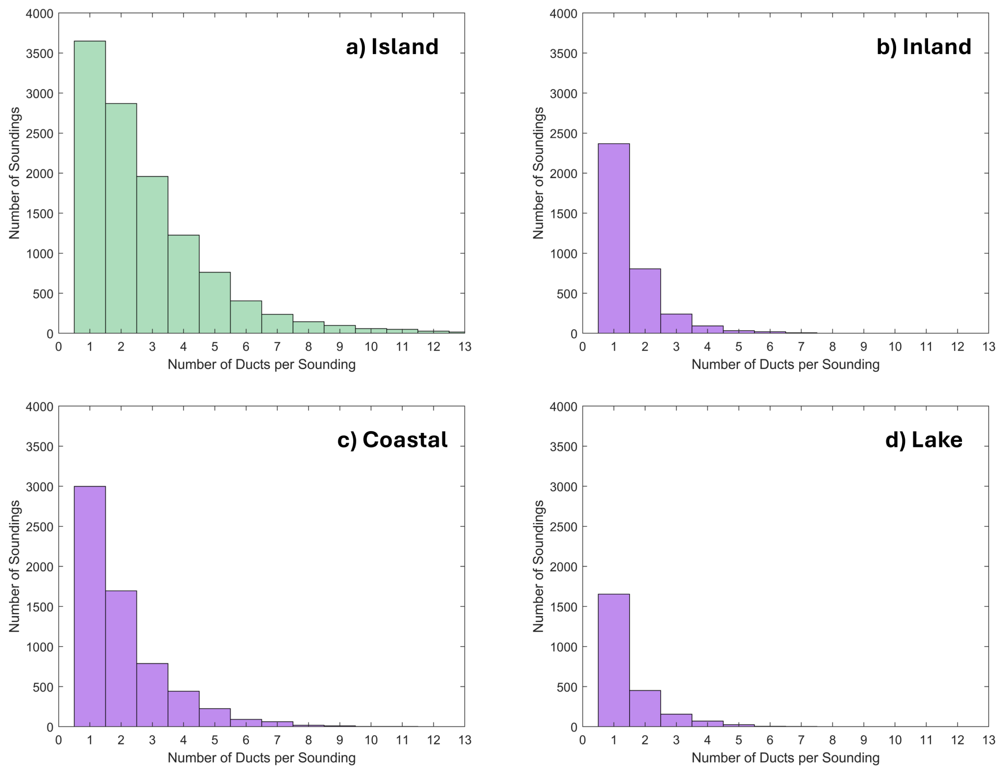

Figure 4. Distribution of number of ducts in a given sounding for a) tropical and subtropical island locations, b) US inland, c) US coastal, and d) Great Lake locations. For island locations, 39 soundings had more than 13 ducts.

Table 3. Median and 10th, 25th, 75th, 90th percentiles for duct characteristics strength, thickness, duct base height, and duct top height for each location type.

	10th	25th	Median	75th	90th
Strength (M)					
Island	2.04	2.66	4.13	7.23	12.40
Coastal	2.10	2.83	4.69	8.69	15.11
Lake	2.03	2.69	4.23	7.46	12.42
Inland	2.05	2.70	4.35	8.19	14.46
Thickness (m)					
Island	52	66	94	156	257
Coastal	55	73	114	191	298
Lake	54	72	104	164	238
Inland	58	76	113	179	276
Duct Base Height (m)					
Island	503	963	1781	2628	3589
Coastal	55	324	874	1730	2720
Lake	41	460	1128	1826	2599
Inland	83	649	1320	2060	2867
Duct Top Height (m)					
Island	627	1098	1935	2750	3689
Coastal	219	512	1018	1887	2720
Lake	177	579	1272	1969	2708
Inland	228	810	1490	2198	2975

2. Results

Most atmospheric profiles at coastal (72%) and island (59%) locations have one or more ducts (Table 1). In comparison, the lake and inland profiles had one or more ducts less than 30% of the time. Multiple ducts per profile are more likely in island locations (Fig. 4). Statistics for duct characteristics by location type are presented in Table 3. Median duct strengths (∼4.1 to 4.7 M) and thicknesses (∼100 m) are similar among the location types. The distributions of duct base altitudes show notable differences among location types, with the median value for islands (1781 m) about 1 km higher in altitude than for coastal (874 m). As a consequence, median duct top altitudes are also about 1 km higher for island as compared to coastal sites. Great Lake and inland locations have median duct base altitudes, 1128 m and 1320 m respectively, at intermediate values between the island and coastal values. The increased height of ducts between US coastal versus subtropical and tropical islands is consistent with the increasing height of the inversion-topped marine boundary layer documented along ship transects that traversed from marine stratocumulus to trade cumulus conditions between Southern California and Hawaii [12].

The interrelationships among the heights, thicknesses, and strength of the ducts observed between the locations are illustrated in Figures 5, 6, and 7. Most ducts are not surface-based (Fig. 5). 75% have tops within the first 3 km of the surface and 75% have thicknesses of 200 m or less (Fig. 6, Table 3). As duct thickness increases > 200 m, the range of duct strengths tends to broaden to include higher value outliers. While thin ducts tend to be weak (M < 10) the high prevalence of weak, thick ducts yields linear correlations that explain less than half the variance between duct strength and and thickness (Fig. 6). There is no meaningful linear correlation between duct strength and height (Fig. 7).

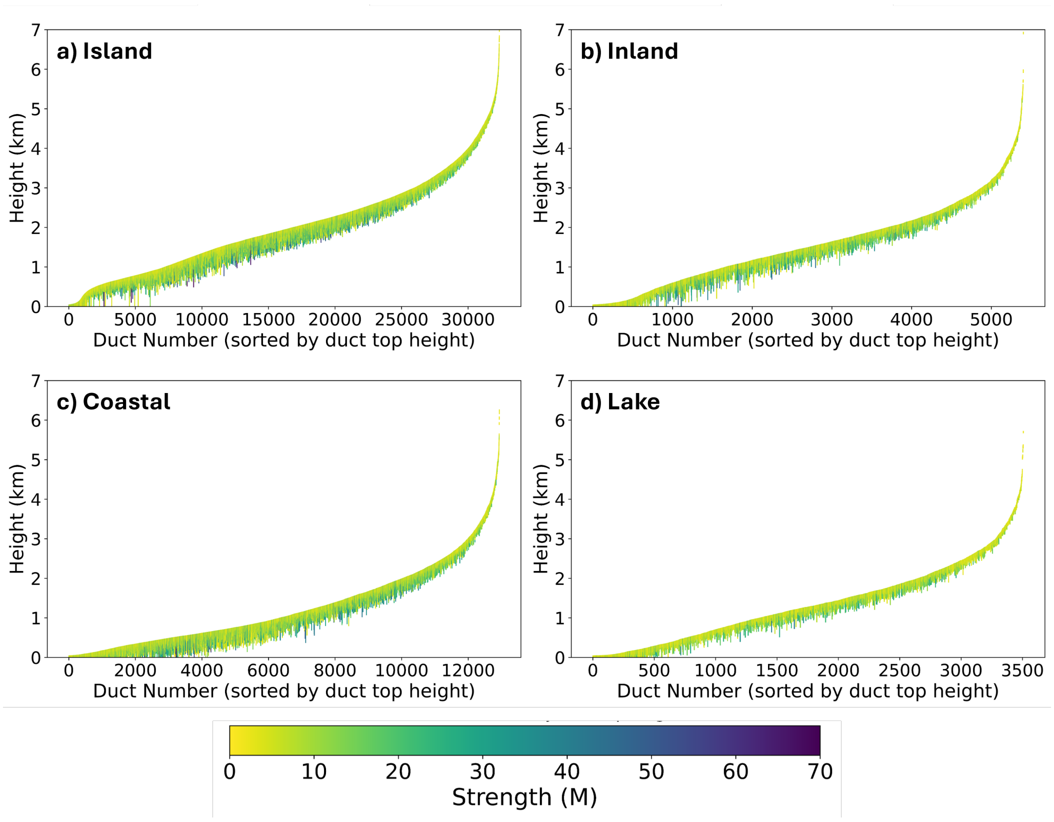

Figure 5. EM duct thickness (vertical length of line) and strength (color-coded) sorted by duct top height for a) tropical and subtropical islands, b) US inland, c) US coastal, and d) Great Lake locations. For island locations, thirteen ducts had duct top heights exceeding 7 km.

The range of surface-based duct strengths is similar to that for elevated ducts (Fig. 7). There are a few outliers with M > 30 in each location category. The surface-based ducts represent a combination of evaporative downdrafts reaching the surface, nocturnal radiation cooling, and sea breezes in coastal, lake, and island locations. Nocturnal radiation inversions are more likely to form on calm, clear nights at inland locations than near bodies of water. The onshore movement of a low layer of cooler ocean air in the afternoon associated with the sea breeze (or a lake breeze) would be conducive to ducting.

The frequency of occurrence of soundings with ducts in different atmospheric layers (surface, between surface and 2 km, and $\geq$ 2 km altitude) is tabulated in Table 4. If a particular sounding had a surface-based duct and one duct above 2 km it would be counted in each of those categories. The island locations stand out with many more soundings containing ducts above 2 km altitude (61%) compared to the other locations (< 31%) which is discussed further in Section 3.

Duct characteristics from US coastal measurements are usually not representative of tropical open ocean conditions. Compared to coastal ducts, the distribution of subtropical and tropical islands ducts heights are shifted to higher altitudes (Fig. 5 and 7, Table 3). Island locations are more likely to have stronger ducts (M > 25) at altitudes above 1 km than coastal locations (Fig. 7). The frequency of surface-based ducts is lower on islands (2%) compared to coastal locations (10%) (Table 4).

3. Discussion

For island locations, while surface-based ducts, and ducts associated with inversions near boundary layer tops were expected, the high prevalence of ducts with bases above boundary layer height (duct base > 2 km altitude) was not expected (Fig. 5, 7, Table 4). Ducts are stable layers so a key question is what are the likely mechanisms producing stable layers

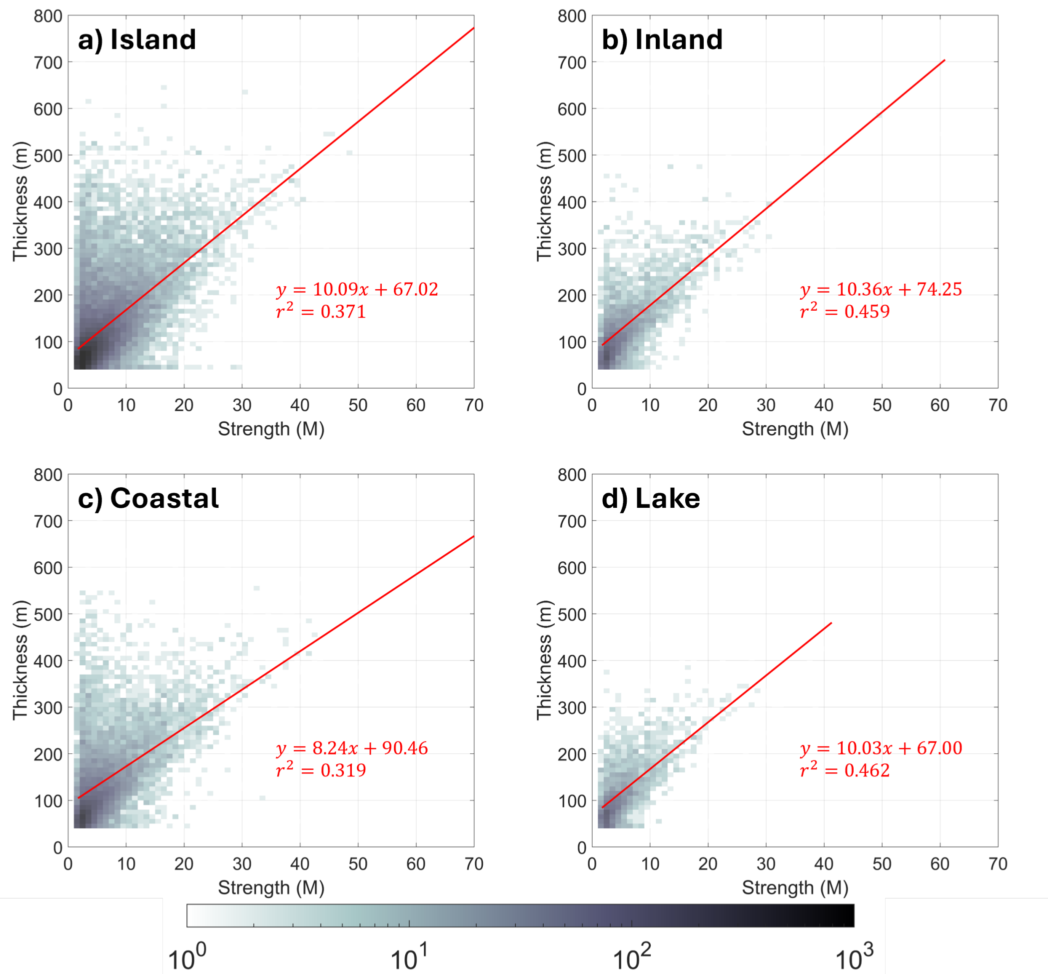

Figure 6. Scatter density plots of duct thickness (m) vs. strength (M) for a) tropical and subtropical islands, b) US inland, c) US coastal, and d) Great Lake locations. Linear regression line (red), corresponding equation, and the coefficient of determination (r^2) are displayed on each subplot. Shading indicates number of samples.

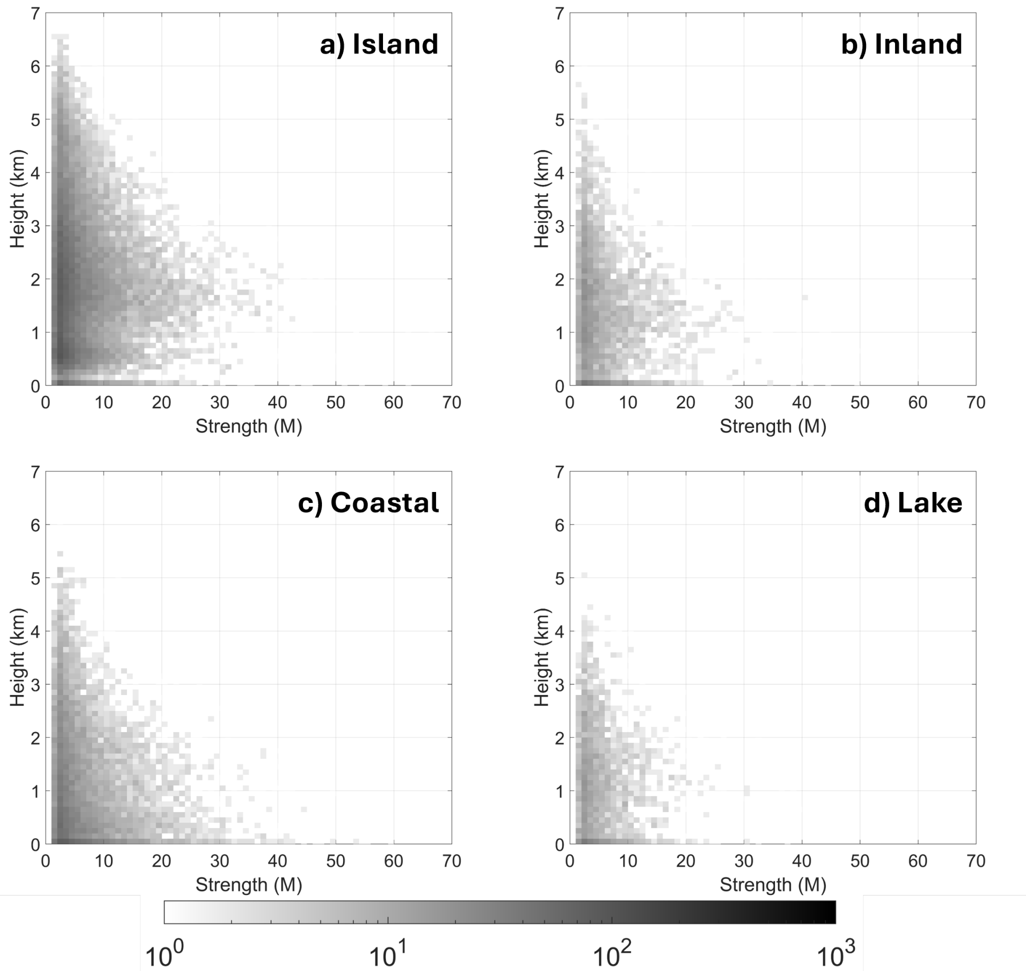

Figure 7. Scatter density plots of duct base height (m) vs. strength (M) for a) tropical and subtropical islands, b) US inland, c) US coastal, and d) Great Lake locations. Shading indicates number of samples.

Table 4. Counts and percentages of duct occurrences in different layers of the atmosphere based on location type. In most circumstances, altitudes > 2 km would be above the boundary layer height [18]. Percentages are relative to total number of soundings with one or more ducts for a location type (Table 1).

Criteria	Island	Coastal	Lake	Inland
Includes a surface-based duct	281 (2.4%)	631 (10.0%)	283 (12.0%)	393 (11.0%)
Includes $\geq$ 1 duct with base >surface and <2 km	8724 (75.6%)	5233 (82.6%)	1829 (77.3%)	2600 (72.9%)
Includes $\geq$ 3 ducts with base >surface and <2 km	1475 (12.8%)	1125 (17.8%)	140 (5.9%)	189 (5.3%)
Includes $\geq$ 1 duct $\geq$ 2 km altitude	7051 (61.1%)	1855 (29.3%)	602 (25.4%)	1120 (31.4%)
Includes $\geq$ 3 ducts $\geq$ 2 km altitude	1637 (14.2%)	132 (2.1%)	25 (1.1%)	51 (1.4%)

$\geq$ 2 km altitude in tropical and subtropical oceanic settings? Subtropical marine regions have persistent large-scale subsidence associated with the downward branch of the Hadley circulation. The subsidence manifests as temperature inversions and humidity gradients yielding trade wind cumulus clouds over warmer oceans and stratocumulus clouds over cooler oceans [19,20]. However, large scale subsidence would not readily explain multiple ducts aloft at different altitudes in the same sounding as illustrated in Figure 3a. In the 24 hours prior to the sounding, Guam hourly METARS reported up to three distinct cloud layers with bases ranging between 600-2700 m. At any one time in a marine cumulus cloud field, clouds are forming and dissipating. Some small cumulus clouds produce precipitation that reaches the surface but most do not. Some cumulus yield virga which will cool and moisten the air just below cloud base. Dry air entrainment dissipates clouds and moistens and cools the immediate vicinity [e.g. 21]. Layer moistening by cumulus cloud dissipation is implicated in the multi-week transition between suppressed (dry) and active (wet) phases of the Madden-Julian oscillation [e.g. 22]. Over hourly to daily time scales, layer moistening by cloud detrainment and virga may have implications for the creation of ∼100 m thick stable layers and potentially ducts if the moisture gradient persists. Determining the physical mechanisms yielding multiple ducts aloft in these settings requires in depth study with more data.

4. Conclusions

Our analysis of more than 49,000 modified refractivity profiles derived from 20 m vertical resolution upper air sounding data complements previous studies on EM duct characteristics based on coarser vertical resolution modeling and observations. By examining a large data set from geographically diverse sites we are able to discern similarities and differences among ducts in different environments. Key findings from observed profiles of modified refractivity including ducts at least 40 m in thickness and with strengths $M \geq 1.7$ are:

- In all location types, elevated ducts are more common than surface-based ducts.
- Median values of duct strengths (M between 4.1 and 4.7) and thicknesses (∼100 m are similar across location types.
- Duct strength tends to increase with increasing duct thickness but this relationship explains less than half of the variance.
- Duct strength and duct base height are not correlated.
- Profiles with one or more ducts are common at tropical and subtropical island (∼60%) and US coastal locations (∼70%) and occur less than 30% of the time at the Great Lakes and US inland sites.

- Notable differences between ducts at tropical and subtropical islands versus US coastal locations include islands having higher median duct base altitudes, higher frequency of stronger ducts at altitudes > 1 km, and lower frequency of of surface-based ducts.
- Tropical and subtropical island locations often exhibit one or more elevated ducts above 2 km altitude in a single profile, a phenomena requiring further investigation.

In the future, the duct inventory we have posted on a public archive can be used as input to radar propagation models to determine the impacts of the observed ducts aloft and at the surface on beam paths for different EM applications.

Author Contributions: Conceptualization, S.Y. and M.M.; methodology, K.B. and M.S.; software, K.B and M.S.; validation, K.B. and S.Y.; resources, M.M.; data curation, K.B. and S.Y.; writing—original draft preparation, S.Y. and M.S.; writing—review and editing, S.Y., M.M., K. B. and M.S.; visualization, S.Y., M.S., and M.M.; supervision, S.Y.; project administration, S.Y.; funding acquisition, S.Y. and M.M. All authors have read and agreed to the published version of the manuscript.

Funding: Research supported by the Office of Naval Research grants N00014-21-1-2166 and N00014-24-1-2216.

Data Availability Statement: Data available in a publicly accessible archive. Upper air sounding data used in this analysis are available from NCEI at https://www.ncei.noaa.gov/data/nws-global-upper-air-bufr/. Data files listing of all identified ducts and their key characteristics at https:doi.org/10.17605/OSF.IO/4THR5.

Acknowledgments: Special thanks to Matt Wilbanks, Tim Whitcomb, Teddy Holt, and James Doyle for their feedback and comments. The views expressed in this article, book, or presentation are those of the authors and do not necessarily reflect the official policy or position of the United States Air Force Academy, the Air Force, the Department of Defense, or the U.S. Government. Approved for public release: distribution unlimited. USAFA-DF-2025-28

Conflicts of Interest: The authors declare no conflicts of interest.

References

1. Kerr, D.E. *Propagation of Short Radio Waves*, 1st ed.; Number 13 in Radiation Laboratory, McGraw-Hill Book Company Inc., 1951.
2. Bean, B.R.; Dutton, E.J. *Radio Meteorology*; Dover Publications, 1966.
3. Rosenthal, J. *Refractive Effects Guidebook*; COMTHIRDFLT TACMEMO 280-1-76, Naval Ocean Systems Center, 1979.
4. Kukushkin, A. *Radio Wave Propagation in the Marine Boundary Layer*; Wiley: New York, 2004.
5. von Engeln, A.; Teixeira, J. A ducting climatology derived from the European Centre for Medium-Range Weather Forecasts global analysis fields. *Journal of Geophysical Research: Atmospheres* **2004**, *109*. _eprint: https://agupubs.onlinelibrary.wiley.com/doi/pdf/10.1029/2003JD004380, https://doi.org/10.1029/2003JD004380.
6. Turton, J.D.; Bennetts, D.A.; Farmer, S.F.G. An introduction to radio ducting. *Meteorological Magazine* **1988**, *117*, 245–254.
7. Brooks, I.M.; Goroch, A.K.; Rogers, D.P. Observations of Strong Surface Radar Ducts over the Persian Gulf. *American Meteorological Society* **1999**, *Volume 38*, 1293–1310. Section: Journal of Applied Meteorology, https://doi.org/https://doi.org/10.1175/1520-0450(1999)038%3C1293:OOSSRD%3E2.0.CO;2.
8. Haack, T.; Burk, S.D. Summertime Marine Refractivity Conditions along Coastal California. *Journal of Applied Meteorology and Climatology* **2001**, *40*, 673–687. Publisher: American Meteorological Society Section: Journal of Applied Meteorology and Climatology, https://doi.org/10.1175/1520-0450(2001)040<0673:SMRCAC>2.0.CO;2.
9. Haack, T.; Wang, C.; Garrett, S.; Glazer, A.; Mailhot, J.; Marshall, R. Mesoscale Modeling of Boundary Layer Refractivity and Atmospheric Ducting. *Journal of Applied Meteorology and Climatology* **2010**, *49*, 2437–2457. Publisher: American Meteorological Society Section: Journal of Applied Meteorology and Climatology, https://doi.org/10.1175/2010JAMC2415.1.
10. Thompson, W.T.; Haack, T. An Investigation of Sea Surface Temperature Influence on Microwave Refractivity: The Wallops-2000 Experiment. *Journal of Applied Meteorology and Climatology* **2011**, *50*, 2319–2337. Publisher: American Meteorological Society Section: Journal of Applied Meteorology and Climatology, https://doi.org/10.1175/JAMC-D-10-05002.1.
11. Cherrett, R.C. Capturing Characteristics of Atmospheric Refractivity Using Observations and Modeling Approaches. Ph.D. Thesis, Naval Postgraduate School, Monterey, California, 2015.
12. Alappattu, D.P.; Wang, Q.; Kalogiros, J. Anomalous propagation conditions over eastern Pacific Ocean derived from MAGIC data. *Radio Science* **2016**, *51*, 1142–1156. _eprint: https://agupubs.onlinelibrary.wiley.com/doi/pdf/10.1002/2016RS005994, https://doi.org/10.1002/2016RS005994.
13. Alappattu, D.P.; Wang, Q.; Yamaguchi, R.T.; Haack, T.; Ulate, M.; Fernando, H.J.; Frederickson, P. Electromagnetic Ducting in the Near-Shore Marine Environment: Results From the CASPER-East Field Experiment. *Journal of Geophysical Research: Atmospheres* **2022**, *127*, e2022JD037423. _eprint: https://agupubs.onlinelibrary.wiley.com/doi/pdf/10.1029/2022JD037423, https://doi.org/10.1029/2022JD037423.
14. Doyle, J.D.; Patel, R.N.; Reynolds, C.; Cobb, A. Impact of Atmospheric Rivers on Electromagnetic Ducting. *Journal of Applied Meteorology and Climatology* **2025**, p. submitted.
15. Saeger, J.T.; Grimes, N.G.; Rickard, H.E.; Hackett, E.E. Evaluation of simplified evaporation duct refractivity models for inversion problems. *Radio Science* **2015**, *50*, 1110–1130. _eprint: https://agupubs.onlinelibrary.wiley.com/doi/pdf/10.1002/2014RS005642, https://doi.org/10.1002/2014RS005642.
16. National Centers for Environmental Information. Global BUFR Data Stream: Upper Air Reports from the National Weather Service Telecommunications Gateway (NWS TG), 2021.
17. World Meteorological Organization. WIS Manuals, 2022.
18. Stull, R.B. *An Introduction to Boundary Layer Meteorology*, softcover reprint of the original 1st ed. 1988 edition ed.; Springer: Dordrecht, 1988.
19. Stevens, B. Atmospheric Moist Convection. *Annual Review of Earth and Planetary Sciences* **2005**, *33*, 605–643. Publisher: Annual Reviews, https://doi.org/10.1146/annurev.earth.33.092203.122658.
20. de Szoeke, S.P.; Verlinden, K.L.; Yuter, S.E.; Mechem, D.B. The Time Scales of Variability of Marine Low Clouds. *Journal of Climate* **2016**, *29*, 6463–6481. https://doi.org/10.1175/JCLI-D-15-0460.1.

21. Gerber, H.E.; Frick, G.M.; Jensen, J.B.; Hudson, J.G. Entrainment, Mixing, and Microphysics in Trade-Wind Cumulus. *Journal of the Meteorological Society of Japan. Ser. II* **2008**, *86A*, 87–106. https://doi.org/10.2151/jmsj.86A.87.
22. Riley, E.M.; Mapes, B.E.; Tulich, S.N. Clouds Associated with the Madden–Julian Oscillation: A New Perspective from CloudSat. *Journal of the Atmospheric Sciences* **2011**, *68*, 3032–3051. Publisher: American Meteorological Society Section: Journal of the Atmospheric Sciences, https://doi.org/10.1175/JAS-D-11-030.1.